

Gate-controlled low carrier density superconductors: Toward the two-dimensional BCS-BEC crossover

Y. Nakagawa,¹ Y. Saito,¹ T. Nojima,² K. Inumaru,³ S. Yamanaka,³ Y. Kasahara,⁴ and Y. Iwasa^{1,5,*}

¹*Quantum-Phase Electronics Center and Department of Applied Physics, The University of Tokyo, Tokyo 113-8656, Japan*

²*Institute for Materials Research, Tohoku University, Sendai 980-8577, Japan*

³*Department of Applied Chemistry, Hiroshima University, Higashi-Hiroshima 739-8527, Japan*

⁴*Department of Physics, Kyoto University, Kyoto 606-8502, Japan*

⁵*RIKEN Center for Emergent Matter Science, Wako 351-0198, Japan*



(Received 28 May 2018; published 24 August 2018)

Superconductivity mostly appears in high carrier density systems and sometimes exhibits common phase diagrams in which the critical temperature T_c continuously develops with carrier density. Superconductivity enhanced in the lightly doped regime has seldom been reported, although it is an ideal direction towards the crossover between Bardeen-Cooper-Schrieffer (BCS) and Bose-Einstein condensate (BEC) limits, where the behavior of Cooper pairs changes dramatically. Here we report transport properties and superconducting gaps in single-crystalline lithium-intercalated layered nitrides (Li_xHfNCl and Li_xZrNCl) down to the low-doping regime, enabled by a combination of ionic gating device and tunneling spectroscopy. Upon the reduction of doping, both systems display the increase of T_c , up to 24.9 K especially in Li_xHfNCl , with the concomitant enhancement of two-dimensionality leading to a pseudogap state below 35.5 K as well as the increase of superconducting coupling strengths $2\Delta/k_B T_c$ reaching 5.9. Such behavior in the carrier density region as low as 10^{20} cm^{-3} indicates that lightly doped two-dimensional superconductors exhibit the unprecedented nature that is distinct from that in conventional superconductors, and offer a new route to access BCS-BEC crossover.

DOI: [10.1103/PhysRevB.98.064512](https://doi.org/10.1103/PhysRevB.98.064512)

I. INTRODUCTION

Superconductivity at very low carrier density is one of the most fascinating phenomena in condensed matter physics. The signature of anomalous electron pairing far above T_c has recently been detected by a single-electron transistor configuration in SrTiO_3 [1]. For another example, FeSe , which is a superconducting semimetal in bulk, shows the magnetic-field-induced transition between two superconducting states [2]. These features are in stark contrast to those in conventional superconductors described by the Bardeen-Cooper-Schrieffer (BCS) theory, and attributed to their small Fermi energies E_F , which are comparable to their superconducting gap Δ . However, the universal pairing mechanism in such a crossover regime of weak-coupling BCS and strong-coupling Bose-Einstein condensate (BEC) limits, where $\Delta/E_F \sim 0.5$ [3], still remains to be resolved. Thus, it is highly desired to explore materials exhibiting superconductivity with low carrier densities as well as to develop a new tool for continuous change of carrier density down to an ultralow level.

Candidate materials that we propose are layered nitrides MNX ($M = \text{Ti}, \text{Zr}, \text{Hf}$; $X = \text{Cl}, \text{Br}, \text{I}$), which are semiconductors and exhibit superconductivity by the intercalation of various metals into their van der Waals gap [Fig. 1(a)] [4–6]. As summarized in Fig. S1 in Supplemental Material Sec. I [7], T_c of both Li intercalated HfNCl and ZrNCl is anomalously high among superconductors with carrier densities lower than

10^{22} cm^{-3} . Furthermore, in the Zr system, T_c increases from 11 to 15 K with the reduction of carrier density [20]. This unique superconducting phase diagram that differs from the dome-shaped ones [21,22], as well as the extremely small γ value determined by the specific-heat measurements [23], raised arguments on potential mechanisms [24–27]. However, such an enhancement has not been reported yet in the Hf system, where we can expect that the higher T_c brings the system closer to the BCS-BEC crossover point than in the case of the Zr system. The obstacle in the previous experiments on layered nitrides is that all of them have been performed only in polycrystalline samples. The grain boundaries and the deficiencies enhance the electron localizations and prevent us from clarifying intrinsic properties especially at the low carrier density limit. Therefore, for further discussion on the pairing properties, the study of single crystals with continuous change of carrier density is crucial.

Here, we demonstrate the precise control of electrochemical intercalation processes in an electric-double-layer transistor (EDLT), employing microscaled single crystals of layered nitrides MNCl , fabricated by mechanical exfoliation. We have designed a device structure that allows us *in situ* measurements of resistivity and tunneling conductance during the electrochemical intercalation process into the bulk preventing surface doping via EDL, and also enables us to access superconductivity in the low carrier density region which cannot be achieved in polycrystalline bulk samples. In this paper, we investigate superconductivity induced by Li interaction in single crystals of both ZrNCl and HfNCl , and find unprecedented superconducting properties, which include concomitant increase of T_c ,

*iwasa@ap.t.u-tokyo.ac.jp

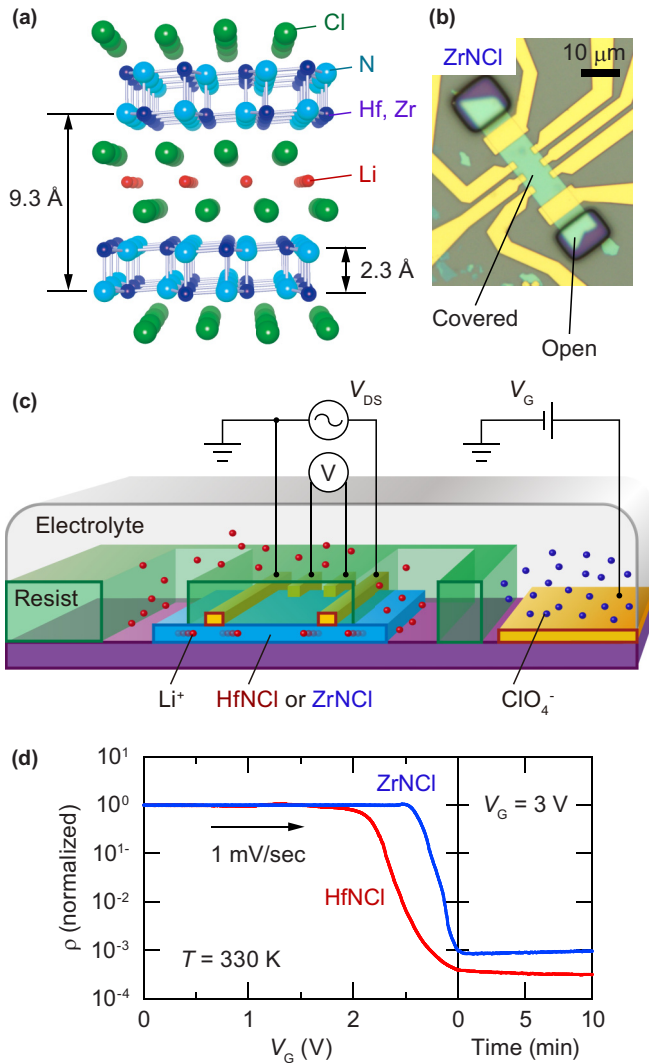


FIG. 1. Ionic-gated intercalation in layered nitrides. (a) Crystal structure of HfNCl (ZrNCl). Hf (Zr)-N double honeycomb layer and trigonal Cl layers are stacked along the c axis. Intercalated Li ions provide electrons to Hf (Zr)-N layers. (b) Optical microscope image of a flake of a layered nitride on a SiO_2/Si substrate patterned into a Hall bar configuration. It is covered with PMMA resist except for the area outside the channel to prevent electrolyte from touching the HfNCl (ZrNCl) surface to form the conducting channel. (c) Schematic of intercalation driven by a positive gate voltage. Li ions were intercalated to the crystal, and the resistance was *in situ* monitored with a small source-drain voltage. (d) Resistivity of ZrNCl (blue) and HfNCl (red) during intercalation at 330 K followed by waiting at $V_G = 3$ V to make it homogeneous. The resistivity decreases because of electron doping.

anisotropy, and coupling strength with reducing the carrier density by controlling the amount of intercalated Li.

The device structure was modified from the conventional EDLT devices [22,28,29] so that the surface carrier doping via EDL is prohibited and only bulk carrier doping via intercalation [30,31] is allowed. Figures 1(b) and 1(c) display an optical image and a schematic diagram of the device used in the present paper, respectively. Because the transport channels of the devices are covered by poly(methyl methacrylate) (PMMA),

EDL between the top surface of the channel and the electrolyte, $\text{LiClO}_4/\text{PEG}$ (polyethylene glycol), cannot be formed while the Li intercalation process proceeds through the open area of both ends of the single crystal. The device was fabricated in a N_2 filled glovebox, which is directly connected to an evaporator to avoid exposure to air. Figure 1(d) shows a typical operation of HfNCl and ZrNCl devices at 330 K. Above a certain critical gate voltage, a sharp decrease in resistance was observed, showing a signature of electron doping through Li intercalation [30,31]. After the decrease of resistance is saturated, we cooled down the device and measured the Hall effect at 150 K, which is far below the melting temperature of the electrolyte (see the Appendix). We assumed that the obtained carrier density is equal to the amount of intercalated Li.

II. RESULTS

Figure 2(a) shows the temperature dependence of resistivity for Li_xHfNCl and Li_xZrNCl single crystals below 40 K. T_c of Li_xZrNCl , defined as the midpoint of the resistive transition, increases from 11.5 to 15.4 K on the reduction of doping from $x = 0.28$ to 0.02 (top panel), being consistent with the bulk measurements on polycrystalline Li_xZrNCl [20]. Unexpectedly, a similar enhancement of T_c was found in Li_xHfNCl , in which T_c increased from 19.4 to 24.9 K by reducing the doping x from 0.28 to 0.03. This value is close to the highest T_c of 25.5 K in layered nitrides, which was observed in cointercalated $\text{Li}_x(\text{THF})_y\text{HfNCl}$ ($x = 0.48$) [5]. The enhanced T_c in the Hf analog is in stark contrast to the results of polycrystalline samples, in which below $x = 0.10$ superconductivity was absent [32]. The limit of superconductivity in polycrystalline Li_xHfNCl is likely due to the electron localization by disorder, and the presently introduced device using single-crystalline samples pushed down the localization limit, enabling us to approach the unprecedented lightly doped regime in Li_xHfNCl .

The $\rho(T)$ curves in Fig. 2(a) show a gradual decrease above T_c . This feature is attributed to the superconducting fluctuation. Importantly, as seen in both panels of Fig. 2(a), the contribution of this fluctuation seemingly depends on x . To quantify the observed excess conductivity, we introduced the Lawrence-Doniach model [33], which describes thermal fluctuation in layered superconductors by considering each layer as a two-dimensional (2D) superconducting sheet interacting with neighbors by the Josephson coupling. In this model, anisotropic parameter $r = 4\xi_z^2/s^2$ is used to describe the strength of interlayer coupling, where ξ_z and s are the out-of-plane coherence length at zero temperature and the interlayer spacing, respectively. Smaller r corresponds to weaker coupling and stronger anisotropy, therefore in the limit of $r \rightarrow 0$ the expression of the fluctuation in this model becomes identical to that in the two-dimensional superconductor. For instance, Aslamazov-Larkin contribution is described as

$$\Delta\sigma_{\text{AL}} = \frac{e^2}{16\hbar s} \frac{1}{\sqrt{\varepsilon(\varepsilon + r)}}, \quad (1)$$

which shows 2D-like ε^{-1} behavior in $r \rightarrow 0$, where ε is the reduced temperature $\ln(T/T_c)$. We performed fitting by using r as a fitting parameter (see Supplemental Material Sec. II [7]); the obtained r is plotted in Fig. 2(b) as a function

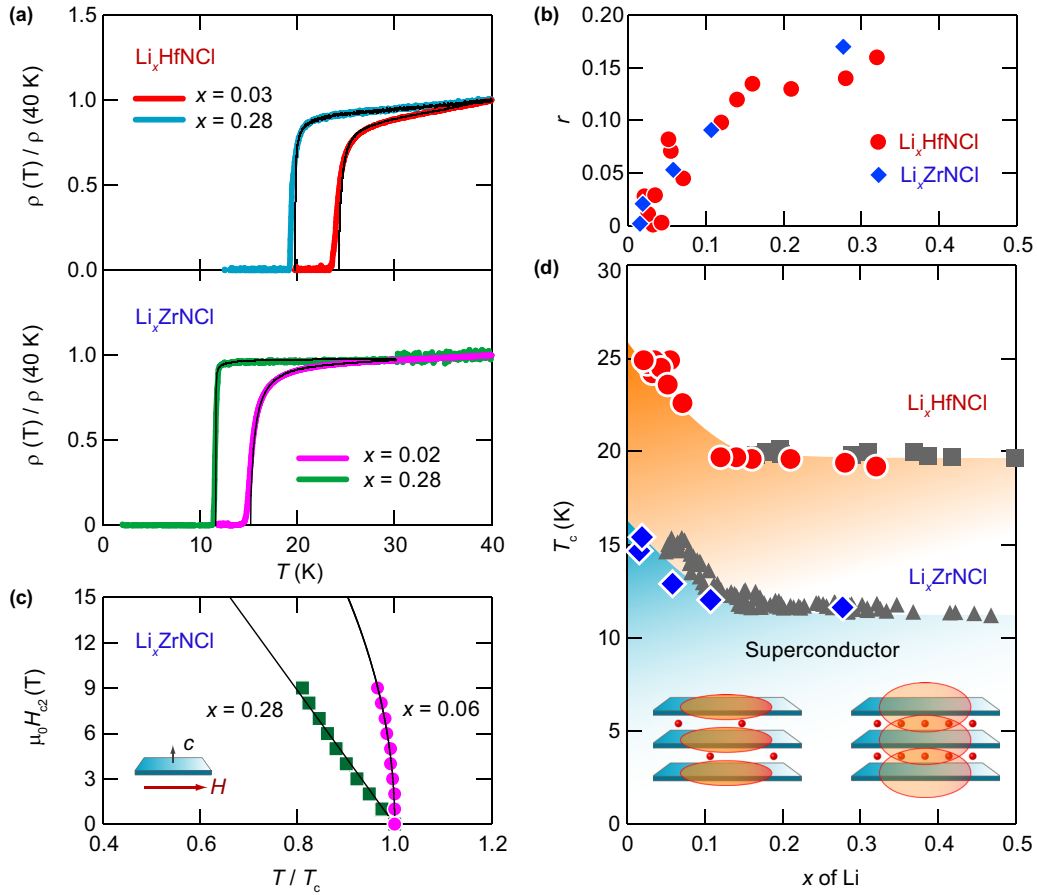


FIG. 2. Doping dependence of T_c and dimensionality. (a) Superconducting transition in Li-doped HfNCl (top) and ZrNCl (bottom). Lower doped samples ($x = 0.02, 0.03$) show higher critical temperatures T_c with larger superconducting fluctuation than higher doped samples ($x = 0.28$). Fits to excess conductivity described by the Lawrence-Doniach model are drawn with solid black curves. (b) Anisotropic parameter in the Lawrence-Doniach model as a function of doping level. Smaller values at light doping level both in Li_xHfNCl (red) and in Li_xZrNCl (blue) correspond to stronger two-dimensionality. (c) In-plane upper critical field H_{c2} as a function of normalized temperature with T_c . Difference of initial rise indicates the change in dimensionality on the reduction of doping from $x = 0.28$ to 0.06. (d) Phase diagram of layered nitrides. Red circles and blue diamonds indicate T_c in single crystals of Li_xHfNCl and Li_xZrNCl , respectively, whereas gray squares and triangles correspond to the polycrystalline samples of Li_xHfNCl and Li_xZrNCl , respectively [20,32]. The common feature is the enhancement of T_c in the lightly doped regime, where superconductivity shows two-dimensionality.

of carrier density both for Li_xZrNCl and for Li_xHfNCl . r systematically decreased with reduction of carrier density, reaching 0.0004 for $x = 0.03$ in Li_xHfNCl , which indicates that the superconductivity is getting highly 2D. If one compares these results with those for high- T_c cuprates, such as less anisotropic YBCO ($r = 0.1$) [34] or highly anisotropic Bi-2212 ($r = 0.004$) [35], obtained r values for the Zr and Hf systems stand out particularly in the low doping limit. Below $x = 0.05$, superconductivity is regarded as practically 2D. Such a doping-induced dimensional crossover, as well as the highly 2D nature in the low doping limit, is an unprecedented property in layered superconductors, which became clear by introducing the *in situ* measurements of intercalations processes on single crystals.

This doping-induced dimensional crossover was also confirmed by the in-plane H_{c2} measurement of Li_xZrNCl , shown in Fig. 2(c). Here H_{c2} was defined as the magnetic field showing a half value of the normal state resistance. In the lightly doped regime ($x = 0.06$), the temperature dependence of H_{c2} shows square root behavior, which is described by the

2D Tinkham model, whereas the linear behavior in the heavily doped regime ($x = 0.28$) is described by the Ginzburg-Landau model for anisotropic three-dimensional superconductors [36]. Even in highly doped Li_xZrNCl ($x = 0.28$), the ratio with the out-of-plane H_{c2} is still as high as 38. This anisotropy parameter is much larger than that obtained in the compressed pellet of 4.5 for $\text{ZrNCl}_{0.7}$ [37], again indicating the crucial importance of using single crystals.

Figure 2(d) displays a T_c versus doping level phase diagram for Li_xHfNCl and Li_xZrNCl . Gray squares and triangles represent the data reported on polycrystalline powders [20,32]. Red circles and blue diamonds are the data obtained in the present experiments. The Zr system shows fair agreement between the polycrystal and single-crystal samples, whereas the Hf analog indicates that the *in situ* measurement in the single-crystal system is able to reach the low carrier density region where T_c is enhanced by nearly 25%.

For elucidating the superconducting coupling strength, we measured tunneling spectra of Li_xHfNCl . Figure 3(a) depicts a schematic energy diagram at the interface between the

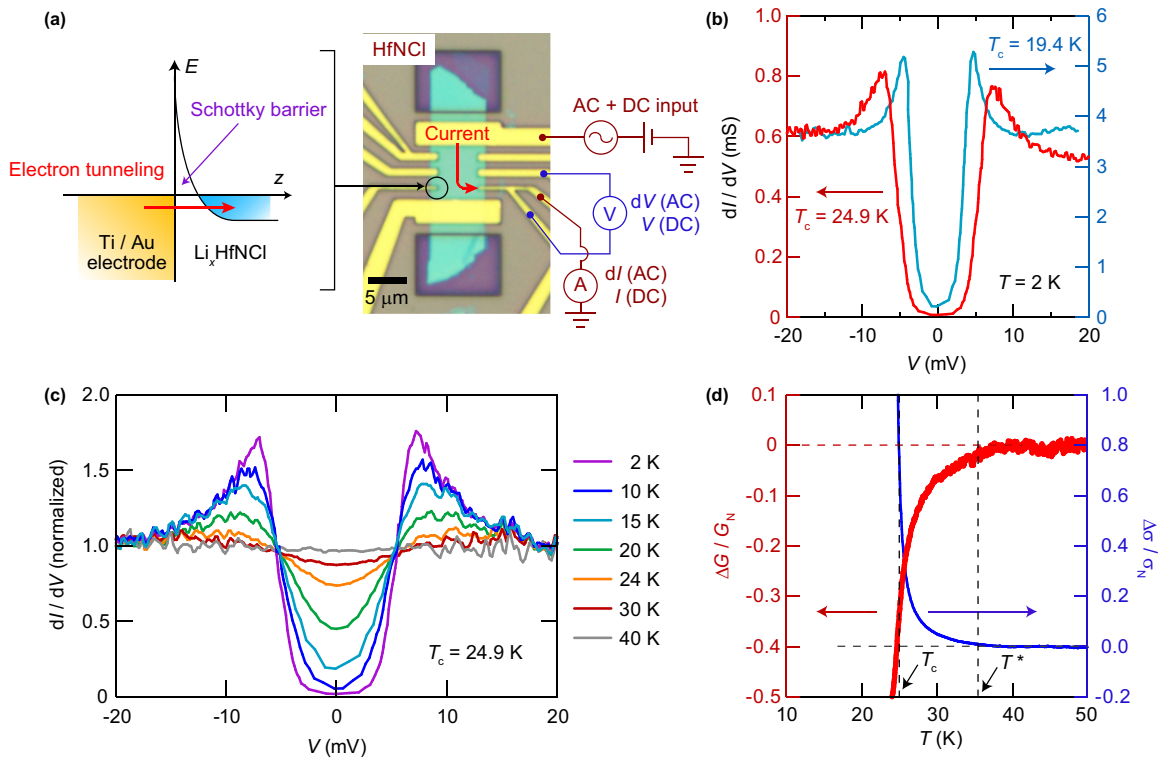


FIG. 3. Tunneling spectroscopy in Li_xHfNCl . (a) Schematic band diagram at the junction between electrode and Li_xHfNCl ; electrons tunnel through the Schottky barrier (left). Illustration of measurement setup; small ac voltage superimposed on dc voltage is applied and the voltage drop at the junction below a thin electrode branch is measured; channel resistance can be measured in the same cool down process (right). (b) Raw data of tunneling spectra in different doping regimes. The different values of the superconducting gap are easily observable, reflecting different T_c of 24.9 (red) and 19.4 K (blue). Difference of the conductance in the normal state appearing at high-biases indicates the different thickness of the Schottky barrier. (c) Tunneling spectra at 2, 10, 15, 20, 24, 30, and 40 K. Upon warming, the gap gets smaller but still exists at 30 K, which is a higher temperature than T_c . The spectra are normalized by using the spectrum at 50 K as a background. (d) Temperature dependence of the zero-bias conductance, or $dI/dV(V = 0)$. The gap starts opening at 35.5 K, which is almost identical to the rising point of excess conductivity, drawn with blue curves.

Ti/Au electrode and Li_xHfNCl . Because the mother compound HfNCl is an insulator before doping, we found that the Schottky barrier remains even after Li intercalation, and works as a tunnel junction [Fig. 3(a)] [38]. By using the formula for the depletion layer [39] (see Supplemental Material Sec. VIII [7]), the Schottky barrier thickness in Li_xHfNCl was estimated to be 0.5 and 0.2 nm for $x = 0.04$ and 0.28, respectively. These values are comparable to the conducting Hf-N layer (0.2 nm), and the effective thickness of the barrier may be enhanced by the insulating Cl layer and van der Waals gap. Such moderate barrier enables us to use electrodes both for tunnel junctions and for the voltage probes in the four-terminal transport measurement. The right side of Fig. 3(a) shows an optical micrograph and the measurement configuration for tunneling spectroscopy. We applied dc and small ac voltage (or current) and measured between the branch of the narrow electrode and a Hall bar. Because the Schottky barrier behaves as a tunneling barrier, dc bias V dependence of differential conductance is described as

$$\frac{dI}{dV}(V) = A \int_{-\infty}^{\infty} N(E) \left(-\frac{\partial f(E + eV)}{\partial V} \right) dE \quad (2)$$

where A is a constant, while $N(E)$ and $f(E)$ are the density of state and the Fermi distribution function, respectively.

Figure 3(b) shows the tunneling spectra at 2 K for Li_xHfNCl with $x = 0.04$ and 0.28, clearly demonstrating the formation of the superconducting gap Δ in $N(E)$ and its variation depending on T_c . Importantly, the data were taken on the same contact of the same sample in different intercalation processes.

Figure 3(c) shows temperature variation of the tunneling spectra for Li_xHfNCl ($x = 0.04$) after subtraction of the channel resistance and normalization by the spectrum at 50 K (see Supplemental Material Sec. III [7]). An interesting feature is that the gap is not completely closed even at 30 K, which is a higher temperature than T_c . The red line in Fig. 3(d) shows the temperature dependence of the normalized zero-bias conductance (ZBC) $\Delta G/G_N$, where $\Delta G = G - G_N$, $G = dI/dV(V = 0)$, and G_N is G under an out-of-plane magnetic field of 9 T. The suppression of ZBC above T_c provides another piece of evidence for the existence of the pseudogap state. The gap opening temperature T^* was determined to be 35.5 K where ZBC is suppressed by 2%. The excess conductivity shown with the blue line in Fig. 3(d) has the onset temperature proximate to T^* , indicating that the observed pseudogap state between T^* and T_c is due to the superconducting fluctuation. The pseudogaplike behavior observed in the nuclear magnetic resonance measurement of the lightly doped Li_xZrNCl ($x = 0.08$) [40] polycrystals likely has the

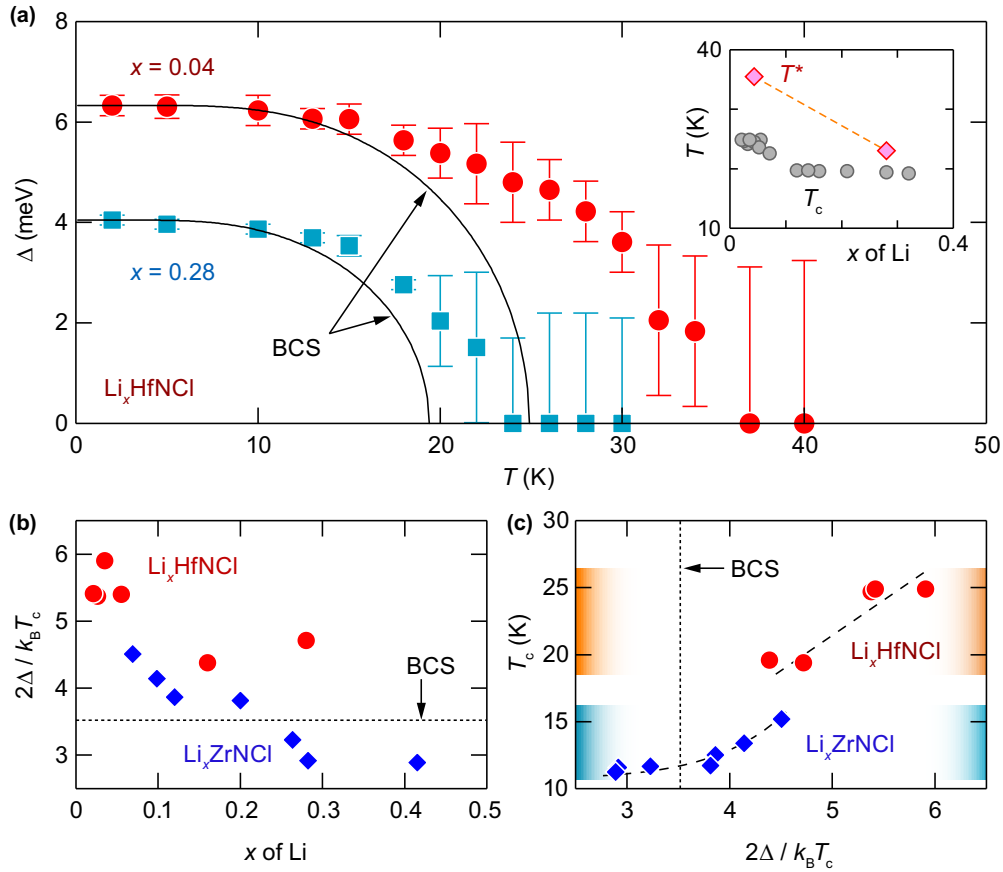


FIG. 4. Superconducting gap and gap ratio in layered nitrides (a) Temperature dependence of Δ for $x = 0.04$ (red circles) and 0.28 (blue squares). Black curves are fits to the BCS-shape function, where T_c was determined by the resistive transition. Error bars represent uncertainties in the fitting (see Supplementary Section VI [7]). The inset shows the doping dependence of T^* and T_c . (b) Doping dependence of gap ratio $2\Delta/k_B T_c$. Red circles indicate the data in single crystals of Li_xHfNCl . The data for polycrystalline Li_xZrNCl (blue diamonds) are taken from the result of specific-heat measurement [44]. They increased upon the reduction of doping, or the enhancement of two-dimensionality, getting beyond the BCS weak-coupling value of 3.53 (dotted line). (c) Critical temperature T_c as a function of $2\Delta/k_B T_c$, or coupling strength. The T_c increases monotonically up to 24.9 K. The data in Li_xZrNCl are taken from the specific-heat measurement [44]. The dotted line and dashed line are the BCS prediction (3.53) and guide to the eye, respectively.

same origin, being different from the electron correlation driven or magnetic correlation driven pseudogap in high- T_c cuprates [21]. We note that the pseudogap is observed also in highly doped Li_xHfNCl ($x = 0.28$), and T^* is 24 K, which is relatively close to T_c [see Supplemental Material Sec. IV [7] and Fig. 4(a) inset]. The temperature range of the pseudogap state is doping dependent.

By fitting the tunneling spectra using Eq. (2) where $N(E)$ is the Dynes function [41], we determined the gap value Δ at each temperature and plotted in Fig. 4(a) for Li_xHfNCl ($x = 0.04$ and 0.28) (see Supplemental Material Sec. VI [7]). Since the gap exists far above T_c , the temperature dependence of Δ cannot be explained by the BCS theory, in which Δ arises at T_c approximately according to a function of $\sqrt{1 - T/T_c}$. The gap opening temperature T^* in the inset of Fig. 4(a) is derived from the midpoint between the lowest zero-gap temperature and the highest finite-gap temperature. $T^* = 35.5$ and 23 K at $x = 0.04$ and 0.28 , respectively, are in good agreement with T^* obtained from ZBC. We calculated doping dependence of $2\Delta/k_B T_c$ at 2 K [Fig. 4(b)], which is the barometer of the coupling strength. Li_xHfNCl is a

member of the strong-coupling superconductor having gap ratios larger than 3.5 in the BCS theory, being consistent with the result of break-junction tunneling spectroscopy in polycrystalline $\text{Li}_{0.5}(\text{THF})_y\text{HfNCl}$ [42] and $\text{HfNCl}_{0.7}$ [43] samples. For the Zr analog, we plotted the data from the specific-heat measurement on polycrystalline samples [44]. In both systems, the ratio increases with reducing the doping level x . Figure 4(c) shows a summary of T_c as a function of $2\Delta/k_B T_c$ both for Li_xHfNCl and Li_xZrNCl systems. A common trend in layered nitrides indicates that the coupling strength well controls the increase of T_c in this system.

III. DISCUSSION

The gap opening below T^* is a very common trend in 2D systems, which is observed in metallic films [45] and $\text{LaAlO}_3/\text{SrTiO}_3$ interfaces [46]. In the latter system, T^* was found to increase with decreasing the carrier density, showing the same carrier density dependence as that in the present system. However, layered nitrides exhibit the opposite T_c - x relation, where both T_c and T^* increase with decreasing the

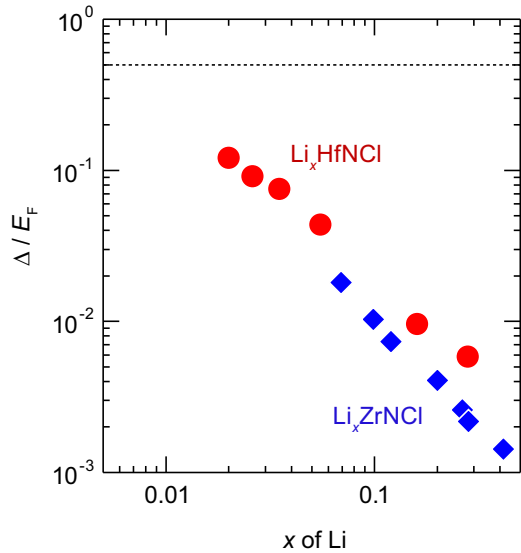


FIG. 5. Doping dependence of the ratio of superconducting gap to Fermi energy. The value of Δ/E_F increases with decreasing the doping level approaching $\Delta/E_F = 0.5$ (dotted line), which indicates the BCS-BEC crossover region [3]. Red circles indicate the present data in Li_xHfNCl , whereas the data in polycrystalline Li_xZrNCl (blue diamonds) are derived from Ref. [44].

carrier density x as seen in the inset of Fig. 4(a). This indicates that an alternative picture can be argued.

An important clue is that the superconducting coupling strength is dramatically enhanced in the low density region. Figure 5 shows the ratio of the superconducting gap and the Fermi energy, Δ/E_F , as a function of x . Both Zr and Hf systems display an increase of Δ/E_F by an order of magnitude with decreasing x . Particularly in Hf analogs, Δ/E_F reaches 0.12 at $x = 0.02$. This is a remarkable enhancement, which is caused by the combined effect of the reduction of carrier density and the concomitant increase of Δ . The increase of T_c with the increase of Δ/E_F as well as increased T^* is reminiscent of the general phase diagram of BCS-BEC crossover, when the coupling strength is increased from the BCS limit. It is also noted that the pseudogap region between T_c and T^* is wider in $x = 0.04$ than in $x = 0.28$. Taking these results into account, we conclude that our system is approaching the BCS-BEC crossover region near $\Delta/E_F \sim 0.5$ [3] by reducing the carrier density with the ionic gating technique.

Recently, the BCS-BEC crossover has been discussed in bulk single-crystal FeSe [2] and magic-angle twisted-bilayer graphene [47], where $\Delta/E_F = 1$ or $T_c/T_F = 0.08$ is observed, respectively. In the latter, the gate control of carrier density is playing a crucial role in a similar manner to the present result. The present system, Li_xHfNCl and Li_xZrNCl , is of particular interest because approaching the BCS-BEC crossover occurs at rather high T_c , and thus may play an important role in the study of BCS-BEC crossover. Regarding the specific pairing mechanism, the present results give a strong constraint to theories. Among many theoretical proposals on superconductivity in Li intercalated HfNCl and ZrNCl systems [24,26,27], the recently reported one taking the valley polarization fluctuation [26,27] at K and K' points into account seems interesting, because it explains the increase of T_c with reducing the carrier

density in 2D multivalley superconductors. It is also noted that the experimentally found gap-opening temperature T^* is close to the predicted T_c of 40 K [27] in Li_xHfNCl , indicating that the theoretically predicted T_c might correspond to the temperature at which the superconducting fluctuation sets in. Such an enhancement is predicted to be universal in 2D doped semiconductors. Not only the layered nitrides, but also other 2D materials like transition-metal dichalcogenides, can be an attractive platform to investigate the BCS-BEC crossover.

To conclude, the voltage control of the electrochemical intercalation process using EDLT devices revealed that superconducting Li_xHfNCl and Li_xZrNCl are potentially a model system to approach the 2D BCS-BEC crossover, in which an increase of T_c and novel exotic aspects of superconductivity are anticipated. We emphasize that gate-controlled nanodevices potentially offer opportunities to access a new state of matter, which is difficult to reach in bulk systems.

ACKNOWLEDGMENTS

We thank M. Nakano and M. Yoshida for discussions and experimental support. This work was supported by Japan Society for the Promotion of Science KAKENHI Grants No. JP25000003, No. JP17J08941, and No. JP15J07681. Y.N. was supported by the Materials Education program for the future leaders in Research, Industry, and Technology.

APPENDIX: MATERIALS AND METHODS

1. Device fabrication

Pristine ZrNCl and HfNCl single crystals were grown by a chemical vapor transport method using vacuum-sealed silica glass tubes and a two-step heating method [48]. They were mechanically exfoliated into thin flakes with tens of nanometers in thickness using the Scotch-tape method, and transferred onto Si/SiO₂ substrates. Ti (5 nm)/Au (70 nm) electrodes were deposited on an isolated thin flake, as well as the gate electrode on the substrate, by the standard electron-beam lithography process. We covered the device with PMMA resist and developed the outer area of the channel. Lithium electrolytes were prepared by dissolving LiClO₄ in PEG. The melting temperatures of PEG used in our experiments, $M = 600$ and 100 000, are 15 and 65 °C, respectively. We added ethanol for easier handling in case of PEG ($M = 100\,000$). After putting a droplet of the electrolyte solution on the flake and the gate electrode, samples were dried in vacuum (lower pressure than 10^{-4} Torr) for 1 hour to eliminate residual moisture, oxygen, and ethanol.

2. Transport measurements

The temperature-dependent resistance was measured with a standard four-probe geometry in a Quantum Design Physical Property Measurement System with two kinds of lock-in amplifiers (Stanford Research Systems Model SR830 DSP and Signal Recovery Model 5210). The gate voltage was applied by a Keithley 2400 source meter at 300 or 330 K under high vacuum. After cooling down to low temperature, the chamber was purged with He. A horizontal rotator probe was used to measure angular dependence of the upper critical field.

3. Tunneling spectroscopy

To input ac and dc excitations, a multifunction generator (NF Corporation WF1974) or ac and dc current source (Keithley Model 6221) were used and both setups output

identical signals. Voltages were probed with an ac lock-in amplifier and a dc voltmeter (Keithley Model 2182A) in the former setup, and with a dc voltmeter (Keithley Model 2182A, differential conductance mode) in the latter setup.

- [1] G. Cheng, M. Tomczyk, S. Lu, J. P. Veazey, M. Huang, P. Irvin, S. Ryu, H. Lee, C.-B. Eom, C. S. Hellberg, and J. Levy, Electron pairing without superconductivity, *Nature (London)* **521**, 196 (2015).
- [2] S. Kasahara, T. Watashige, T. Hanaguri, Y. Kohsaka, T. Yamashita, Y. Shimoyama, Y. Mizukami, R. Endo, H. Ikeda, K. Aoyama, T. Terashima, S. Uji, T. Wolf, H. v. Löhneysen, T. Shibauchi, and Y. Matsuda, Field-induced superconducting phase of FeSe in the BCS-BEC cross-over, *Proc. Natl. Acad. Sci. USA* **111**, 16309 (2014).
- [3] M. Randeria and E. Taylor, Crossover from Bardeen-Cooper-Schrieffer to Bose-Einstein condensation and the unitary Fermi gas, *Annu. Rev. Condens. Matter Phys.* **5**, 209 (2014).
- [4] S. Yamanaka, H. Kawaji, K.-i. Hotehama, and M. Ohashi, A new layer-structured nitride superconductor. Lithium-intercalated β -zirconium nitride chloride, Li_xZrNCl . *Adv. Mater.* **8**, 771 (1996).
- [5] S. Yamanaka, K.-i. Hotehama, and H. Kawaji, Superconductivity at 25.5 K in electron-doped layered hafnium nitride, *Nature (London)* **392**, 580 (1998).
- [6] Y. Kasahara, K. Kuroki, S. Yamanaka, and Y. Taguchi, Unconventional superconductivity in electron-doped layered metal nitride halides MNX ($M = \text{Ti, Zr, Hf}$; $X = \text{Cl, Br, I}$), *Physica C* **514**, 354 (2015).
- [7] See Supplemental Material at <http://link.aps.org/supplemental/10.1103/PhysRevB.98.064512>, which includes Refs. [8–19], for comparison with other superconductors, additional tunneling spectra, details about the analysis of conductivity and tunneling spectra, evaluation of the resist cover, and estimation of the thickness of the tunneling barrier.
- [8] J. F. Schooley, W. R. Hosler, E. Ambler, J. H. Becker, M. L. Cohen, and C. S. Koonce, Dependence of the Superconducting Transition Temperature on Carrier Concentration in Semiconducting SrTiO_3 , *Phys. Rev. Lett.* **14**, 305 (1965).
- [9] R. A. Hein, J. W. Gibson, R. Mazelsky, R. C. Miller, and J. K. Hulm, Superconductivity in Germanium Telluride, *Phys. Rev. Lett.* **12**, 320 (1964).
- [10] Y. Matsushita, P. A. Wianeci, A. T. Sommer, T. H. Geballe, and I. R. Fisher, Type II superconducting parameters of Tl-doped PbTe determined from heat capacity and electronic transport measurements, *Phys. Rev. B* **74**, 134512 (2006).
- [11] Y. S. Hor, A. J. Williams, J. G. Checkelsky, P. Roushan, J. Seo, Q. Xu, H.W. Zandbergen, A. Yazdani, N.P. Ong, and R. J. Cava, Superconductivity in $\text{Cu}_x\text{Bi}_2\text{Se}_3$ and its Implications for Pairing in the Undoped Topological Insulator, *Phys. Rev. Lett.* **104**, 057001 (2010).
- [12] H. Takagi, T. Ido, S. Ishibashi, M. Uota, S. Uchida, and Y. Tokura, Superconductor-to-nonsuperconductor transition in $(\text{La}_{1-x}\text{Sr}_x)_2\text{CuO}_4$ as investigated by transport and magnetic measurements, *Phys. Rev. B* **40**, 2254 (1989).
- [13] E. Bustarret, J. Kačmarčík, C. Marcenat, E. Gheeraert, C. Cytermann, J. Marcus, and T. Klein, Dependence of the Superconducting Transition Temperature on the Doping Level in Single-Crystalline Diamond Films, *Phys. Rev. Lett.* **93**, 237005 (2004).
- [14] T. Terashima, N. Kikugawa, A. Kiswandhi, E.-S. Choi, J. S. Brooks, S. Kasahara, T. Watashige, H. Ikeda, T. Shibauchi, Y. Matsuda, T. Wolf, A. E. Böhmer, F. Hardy, C. Meingast, H. v. Löhneysen, M. Suzuki, R. Arita, and S. Uji, Anomalous Fermi surface in FeSe seen by Shubnikov–de Haas oscillation measurements, *Phys. Rev. B* **90**, 144517 (2014).
- [15] J. Axnäs, W. Holm, Y. Eltsev, and Ö. Rapp, Sign Change of c -Axis Magnetoconductivity in $\text{YBa}_2\text{Cu}_3\text{O}_{7-\delta}$ Single Crystals, *Phys. Rev. Lett.* **77**, 2280 (1996).
- [16] M. Hikita and M. Suzuki, Fluctuation conductivity and normal resistivity in $\text{YBa}_2\text{Cu}_3\text{O}_y$, *Phys. Rev. B* **41**, 834 (1990).
- [17] T. Takano, Y. Kasahara, T. Oguchi, I. Hase, Y. Taguchi, and Y. Iwasa, Doping variation of optical properties in ZrNCl superconductors. *J. Phys. Soc. Jpn* **80**, 023702 (2011).
- [18] A. S. Botana and W. E. Pickett, Dielectric response of electron-doped ionic superconductor Li_xZrNCl , *Phys. Rev. B* **90**, 125145 (2014).
- [19] J. Liu, X.-B. Li, D. Wang, H. Liu, P. Peng, and L.-M. Liu, Single-layer group-IVB nitride halides as promising photocatalysts, *J. Mater. Chem. A* **2**, 6755 (2014).
- [20] Y. Taguchi, A. Kitora, and Y. Iwasa, Increase in T_c Upon Reduction of Doping in Li_xZrNCl Superconductors, *Phys. Rev. Lett.* **97**, 107001 (2006).
- [21] B. Keimer, S. A. Kivelson, M. R. Norman, S. Uchida, and J. Zaanen, From quantum matter to high-temperature superconductivity in copper oxides, *Nature (London)* **518**, 179 (2015).
- [22] J. T. Ye, Y. J. Zhang, R. Akashi, M. S. Bahramy, R. Arita, and Y. Iwasa, Superconducting dome in a gate-tuned band insulator, *Science* **338**, 1193 (2012).
- [23] Y. Taguchi, M. Hisakabe, and Y. Iwasa, Specific Heat Measurement of the Layered Nitride Superconductor Li_xZrNCl , *Phys. Rev. Lett.* **94**, 217002 (2005).
- [24] K. Kuroki, Spin-fluctuation-mediated $d + id'$ pairing mechanism in doped $\beta - MNCl$ ($M = \text{Hf, Zr}$) superconductors, *Phys. Rev. B* **81**, 104502 (2010).
- [25] R. Akashi, K. Nakamura, R. Arita, and M. Imada, High-temperature superconductivity in layered nitrides $\beta - \text{Li}_x\text{MNCl}$ ($M = \text{Ti, Zr, Hf}$): Insights from density functional theory for superconductors, *Phys. Rev. B* **86**, 054513 (2012).
- [26] M. Calandra, P. Zocante, and F. Mauri, Universal Increase in the Superconducting Critical Temperature of Two-Dimensional Semiconductors at Low Doping by the Electron-Electron Interaction, *Phys. Rev. Lett.* **114**, 077001 (2015).
- [27] B. Pamuk, F. Mauri, and M. Calandra, High- T_c superconductivity in weakly electron-doped HfNCl, *Phys. Rev. B* **96**, 024518 (2017).
- [28] J. T. Ye, S. Inoue, K. Kobayashi, Y. Kasahara, H. T. Yuan, H. Shimotani, and Y. Iwasa, Liquid-gated interface superconductivity on an atomically flat film, *Nature Mater.* **9**, 125 (2010).

- [29] Y. Saito, Y. Kasahara, J. T. Ye, Y. Iwasa, and T. Nojima, Metallic ground state in an ion-gated two-dimensional superconductor, *Science* **350**, 409 (2015).
- [30] Y. Yu, F. Yang, X. F. Lu, Y. J. Yan, Y.-H. Cho, L. Ma, X. Niu, S. Kim, Y.-W. Son, D. Feng, S. Li, S.-W. Cheong, X. H. Chen, and Y. Zhang, Gate-tunable phase transitions in thin flakes of 1T-TaS₂, *Nature Nanotech.* **10**, 270 (2015).
- [31] W. Shi, J. T. Ye, Y. J. Zhang, R. Suzuki, M. Yoshida, J. Miyazaki, N. Inoue, Y. Saito, and Y. Iwasa, Superconductivity series in transition metal dichalcogenides by ionic gating, *Sci. Rep.* **5**, 12534 (2015).
- [32] T. Takano, T. Kishiume, Y. Taguchi, and Y. Iwasa, Interlayer-Spacing Dependence of T_c in $\text{Li}_x\text{M}_y\text{HfNCl}$ (M : Molecule) Superconductors, *Phys. Rev. Lett.* **100**, 247005 (2008).
- [33] A. Larkin and A. Varlamov, *Theory of Fluctuations in Superconductors* (Clarendon, Oxford, 2005).
- [34] B. Oh, K. Char, A. D. Kent, M. Naito, M. R. Beasley, T. H. Geballe, R. H. Hammond, A. Kapitulnik, and J. M. Graybeal, Upper critical field, fluctuation conductivity, and dimensionality of $\text{YBa}_2\text{Cu}_3\text{O}_{7-x}$, *Phys. Rev. B* **37**, 7861 (1988).
- [35] A. Pomar, M. V. Ramallo, J. Mosqueira, C. Torrón, and F. Vidal, Fluctuation-induced in-plane conductivity, magnetoconductivity, and diamagnetism of $\text{Bi}_2\text{Sr}_2\text{CaCu}_2\text{O}_8$ single crystals in weak magnetic fields, *Phys. Rev. B* **54**, 7470 (1996).
- [36] M. Tinkham, *Introduction to Superconductivity*, 2nd ed. (Dover, New York, 2004).
- [37] H. Tou, Y. J. Tanaka, M. Sera, Y. Taguchi, T. Sasaki, Y. Iwasa, L. Zhu, and S. Yamanaka, Upper critical field in the electron-doped layered superconductor $\text{ZrNCl}_{0.7}$: Magnetoresistance studies, *Phys. Rev. B* **72**, 020501 (2005).
- [38] C. B. Duke, *Tunneling in Solids* (Academic, New York, 1969).
- [39] S. M. Sze, *Semiconductor Devices: Physics and Technology* (Wiley, New York, 1985).
- [40] H. Kotegawa, S. Oshiro, Y. Shimizu, H. Tou, Y. Kasahara, T. Kishiume, Y. Taguchi, and Y. Iwasa, Strong suppression of coherence effect and appearance of pseudogap in the layered nitride superconductor Li_xZrNCl : ^{91}Zr - and ^{15}N -NMR studies, *Phys. Rev. B* **90**, 020503 (2014).
- [41] R. C. Dynes, V. Narayanamurti, and J. P. Garno, Direct Measurement of Quasiparticle-Lifetime Broadening in a Strong-Coupled Superconductor, *Phys. Rev. Lett.* **41**, 1509 (1978).
- [42] T. Ekino, T. Takasaki, T. Muranaka, H. Fujii, J. Akimitsu, and S. Yamanaka, Tunneling spectroscopy of MgB_2 and $\text{Li}_{0.5}(\text{THF})_y\text{HfNCl}$, *Physica B* **328**, 23 (2003).
- [43] T. Takasaki, T. Ekino, and S. Yamanaka, Tunneling spectroscopy of layered nitride superconductors $\text{MNCl}_{0.7}$ ($M = \text{Hf}$ and Zr), *Physica C* **445-448**, 77 (2006).
- [44] Y. Kasahara, T. Kishiume, T. Takano, K. Kobayashi, E. Matsumoto, H. Onodera, K. Kuroki, Y. Taguchi, and Y. Iwasa, Enhancement of Pairing Interaction and Magnetic Fluctuations Toward a Band Insulator in an Electron-Doped Li_xZrNCl Superconductor, *Phys. Rev. Lett.* **103**, 077004 (2009).
- [45] B. Sacépé, C. Chapelier, T. I. Baturina, V. M. Vinokur, M. R. Baklanov, and M. Sanquer, Pseudogap in a thin film of a conventional superconductor, *Nature Commun.* **1**, 140 (2010).
- [46] C. Richter, H. Boschker, W. Dietsche, E. Fillis-Tsirakis, R. Jany, F. Loder, L. F. Kourkoutis, D. A. Muller, J. R. Kirtley, C. W. Schneider, and J. Mannhart, Interface superconductor with gap behaviour like a high-temperature superconductor, *Nature (London)* **502**, 528 (2013).
- [47] Y. Cao, V. Fatemi, S. Fang, K. Watanabe, T. Taniguchi, E. Kaxiras, and P. Jarillo-Herrero, Unconventional superconductivity in magic-angle graphene superlattices, *Nature (London)* **556**, 43 (2018).
- [48] S. Yamanaka, High- T_c superconductivity in electron-doped layer structured nitrides, *Annu. Rev. Mater. Sci.* **30**, 53 (2000).